Paper No. 241. (quote when citing this article)
Eleventh World Conference on Earthquake Engineering
ISBN: 0 08 042822 3

IMPULSE FUNCTION OF DYNAMIC STIFFNESS OF SOIL

N. YOSHIDA

Department of Structural Engineering, Hiroshima University,
1-4-1, Kagamiyama, Higashi-Hiroshima 739, Japan

ABSTRACT

The impulse function of dynamic stiffness of soil and its convolution integral are calculated to evaluate the dynamic interaction forces between soil and structures in time domain. This paper formulates three kinds of convolution representation for the dynamic interaction force and the related transform rules with causality. Finally a new method to express the impulse function is presented by using a discrete Hilbert transform and the causal inverse fast Fourier transform together with the complex exponential algorithm.

KEYWORDS

Dynamic sub-structure method; Impulse function; Dynamic stiffness of soil; Causality; Fourier transform; Hilbert transform; Complex exponential algorithm.

INTRODUCTION

The impulse function of the dynamic stiffness of soil is used in the time domain analysis of soil-structure interaction (Wolf and Obernhuber, 1985; Wolf and Darbre, 1986; Wijeyewickrema and Keer, 1987; Wolf and Motosaka, 1989). This paper presents a method to obtain the analytical representation for the impulse function. The dynamic stiffness of soil is generally obtained by numerical analysis such as the boundary integral equation method or its hybrid method with the finite element method. The dynamic stiffness can be decomposed into the regular and the singular parts in the three types (Yoshida *et al*, 1986; Hayashi and Katukura, 1990). The singular part is independent from frequency, evaluated at the frequency of zero or infinity so that the regular part which is varied with the frequency may be gradually decreased to zero at infinity. If the real part of the dynamic stiffness could not be obtained, the real part of the regular part is approximately calculated from its imaginary part in frequency domain (Yoshida *et al*, 1986) in order to satisfy the causality by using a discrete Hilbert transform (Simon and Tomlinson, 1984).

Applying the causal inverse fast Fourier transform (Hayashi and Katukura, 1990) to this real part, the impulse function of the dynamic stiffness of soil is obtained as a large amount of data on the time axis. This

requires a huge memory size, and so makes it difficult to calculate the convolution integrals representing the interaction force by a small computer. The impulse data is replaced to a series of analytical functions approximately by using the complex exponential algorithm which is the curve-fitting technique based on Prony's method (Brown *et al*, 1979) and also by using a generalized inverse technique. The obtained impulse functions strictly satisfy the causality and are perfectly stable. The number of numerical factors contained in the exponential functions and their amplitude is quite a few. Therefore, this method makes it easy to calculate the convolution integrals in high speed and to reduce the storage of information on the impulse function compared with the ordinary inverse fast Fourier transform. Finally numerical results for a simple model are shown and the validity of the proposed method is examined.

DYNAMIC SUB-STRUCTURE METHOD IN TIME DOMAIN

The equations of motion for the inner field V_I containing the structures (Fig.1) can be discretized by the numerical method such as the finite element method as follows:

$$\begin{bmatrix}[M_{SS}] & [M_{SB}]\\ [M_{BS}] & [M_{BB}]\end{bmatrix}\begin{Bmatrix}\{\ddot{u}_S(t)\}\\ \{\ddot{u}_B(t)\}\end{Bmatrix}+\begin{bmatrix}[C_{SS}] & [C_{SB}]\\ [C_{BS}] & [C_{BB}]\end{bmatrix}\begin{Bmatrix}\{\dot{u}_S(t)\}\\ \{\dot{u}_B(t)\}\end{Bmatrix}+\begin{bmatrix}[K_{SS}] & [K_{SB}]\\ [K_{BS}] & [K_{BB}]\end{bmatrix}\begin{Bmatrix}\{u_S(t)\}\\ \{u_B(t)\}\end{Bmatrix}=\begin{Bmatrix}\{0\}\\ -\{R(t)\}\end{Bmatrix} \tag{1}$$

in which $\{u\}$ and $\{R\}$ denote the displacement vector and the dynamic interaction force vector in time domain on the pseudo boundary surface S_B respectively.

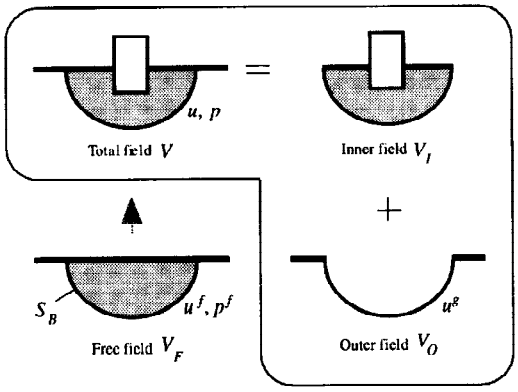

Fig.1 Substructure model

$\{R(t)\}$ is represented by the inverse Fourier transform or the convolution integral using the dynamic stiffness matrix $[S]$ obtained by the boundary integral equation method or the transmitting boundary representation as follows:

$$\{R(t)\}=\frac{1}{2\pi}\int_{-\infty}^{\infty}[S(\omega)]\{u(\omega)\}e^{i\omega t}d\omega=\int_0^t[S(t-\tau)]\{u(\tau)\}d\tau \tag{2}$$

in which $\{u\}$ denotes the relative displacements from the free motion $\{u_B^g\}$ in the outer field V_O

$$\{u(\omega)\}=\{u_B(\omega)\}-\{u_B^g(\omega)\}. \tag{3}$$

The free surface condition on S_B in the outer field V_O is given by

$$\{p_B^g(\omega)\}=\{p_B^f(\omega)\}+[S(\omega)]\left(\{u_B^g(\omega)\}-\{u_B^f(\omega)\}\right)=0 \tag{4}$$

or

in which $\{p\}$ is the surface traction and the super suffix f denotes the free field with no structures.

From all of the above equations, the fundamental equations in the dynamic sub-structure method are formulated:

$$\begin{bmatrix}[M_{SS}] & [M_{SB}]\\ [M_{BS}] & [M_{BB}]\end{bmatrix}\begin{Bmatrix}\{\ddot{u}_S(t)\}\\ \{\ddot{u}_B(t)\}\end{Bmatrix}+\begin{bmatrix}[C_{SS}] & [C_{SB}]\\ [C_{BS}] & [C_{BB}]+[c^n]\end{bmatrix}\begin{Bmatrix}\{\dot{u}_S(t)\}\\ \{\dot{u}_B(t)\}\end{Bmatrix}+\begin{bmatrix}[K_{SS}] & [K_{SB}]\\ [K_{BS}] & [K_{BB}]+[k^n]\end{bmatrix}\begin{Bmatrix}\{u_S(t)\}\\ \{u_B(t)\}\end{Bmatrix}$$

$$+\begin{Bmatrix}\{0\}\\ \int_0^t[S_l^r(t-\tau)]d^{l-1}\{u_B(\tau)\}/d\tau^{l-1}\cdot d\tau\end{Bmatrix}=\begin{Bmatrix}\{0\}\\ [c^n]\{\dot{u}_B^g(t)\}+[k^n]\{u_B^g(t)\}+\int_0^t[S_l^r(t-\tau)]d^{l-1}\{u_B^g(\tau)\}/d\tau^{l-1}\cdot d\tau\end{Bmatrix}. \quad (6)$$

$[S(\omega)]$ can be decomposed into the regular and the singular parts in the three following ways:

$$[S(\omega)]=[S_l^n]+[S_l^r(\omega)](\mathrm{i}\omega)^{l-1} \quad : l=1,2,3 \quad (7)$$

where

$[S(\omega)]=[k(\omega)]+\mathrm{i}\omega[c(\omega)]$,
$[S_l^n]=[k^n]+\mathrm{i}\omega[c^n]$: singular part,
$[S_l^r(\omega)]=[k^r(\omega)]+\mathrm{i}\omega[c^r(\omega)]$: regular part.

Table 1. Regular and singular parts of $[S(\omega)]$

	$l=1$	$l=2$	$l=3$
$[k^n]$	$[k(\infty)]$	$[k(0)]$	$[k(0)]$
$[c^n]$	$[c(\infty)]$	$[c(\infty)]$	$[c(0)]$
$[k^r(\omega)]$	$[k(\omega)]-[k(\infty)]$	$[c(\omega)]-[c(\infty)]$	$\dfrac{[k(0)]-[k(\omega)]}{\omega^2}$
$[c^r(\omega)]$	$[c(\omega)]-[c(\infty)]$	$\dfrac{[k(0)]-[k(\omega)]}{\omega^2}$	$\dfrac{[c(0)]-[c(\omega)]}{\omega^2}$

Each element of $[S_l^n]$ and $[S_l^r(\omega)]$ is shown in Table 1.

Substituting equation (7) in equation (2) leads to

$$\{R(t)\}=[k^n]\{u(t)\}+[c^n]\frac{d}{dt}\{u(t)\}+\int_0^t[S_l^r(t-\tau)]\frac{d^{l-1}}{d\tau^{l-1}}\{u(\tau)\}d\tau. \quad (8)$$

CAUSAL INVERSE FOURIER TRANSFORM

Causality

If the impulse function of the regular part is real and satisfies the causality $\left([S_l^r(t<0)]=0\right)$, both $[k^r(\omega)]$ and $[c^r(\omega)]$ satisfy the equations

$$[k^r(\omega)] = -\frac{1}{\pi}\mathrm{P}\int_{-\infty}^{\infty}\frac{z[c^r(z)]}{z-\omega}dz = -\frac{2}{\pi}\mathrm{P}\int_0^{\infty}\frac{z^2[c^r(z)]}{z^2-\omega^2}dz \tag{9}$$

$$[c^r(\omega)] = \frac{1}{\pi\omega}\mathrm{P}\int_{-\infty}^{\infty}\frac{[k^r(z)]}{z-\omega}dz = \frac{2}{\pi}\mathrm{P}\int_0^{\infty}\frac{[k^r(z)]}{z^2-\omega^2}dz, \tag{10}$$

known as the Hilbert transform where $\mathrm{P}\int$ denotes the principal value of the integral.

In this case $[S_l^r(t)]$ can be expressed only by $[k^r(\omega)]$ or $[c^r(\omega)]$ in the following form

$$[S_l^r(t)] = \frac{1}{2\pi}\int_{-\infty}^{\infty}[S_l^r(\omega)]e^{\mathrm{i}\omega t}d\omega = 4U(t)\cdot\mathrm{Re}\left[\frac{1}{2\pi}\int_0^{\infty}[k^r(\omega)]e^{\mathrm{i}\omega t}d\omega\right]$$

$$= 4U(t)\cdot\mathrm{Re}\left[\frac{1}{2\pi}\int_0^{\infty}\mathrm{i}\omega[c^r(\omega)]e^{\mathrm{i}\omega t}d\omega\right] \tag{11}$$

where $U(t)=1$ $(t>0)$, 0 $(t<0)$ denotes the step function. The equations above are called the causal Fourier transform.

Causal Inverse Fast Fourier Transform (CIFFT)

Equations (11) can be evaluated at a series of discrete points $t_m = m\Delta T(m=0,1,\cdots,N/2)$ as

$$S_l^r(t_m) = \frac{4}{N\Delta T}\mathrm{Re}\left[\frac{1}{2}k^r(0) + \sum_{j=1}^{N/2-1}k^r(j\Delta\omega)e^{\mathrm{i}(2\pi jm/N)} + \frac{1}{2}k^r(\frac{N}{2}\Delta\omega)e^{\mathrm{i}\pi m}\right] \tag{12}$$

where $\Delta\omega = \dfrac{2\pi}{T} = \dfrac{2\pi}{N\Delta T}$. A set of data produced by adding $N/2-1$ zeros to the discrete values in equation (12)

$$\frac{4}{N\Delta T}\left\{\frac{1}{2}k^r(0),\ k^r(\Delta\omega),\ \cdots,\ \frac{1}{2}k^r(\frac{N}{2}\Delta\omega),\ \underbrace{0,\ \cdots,\ 0}_{N/2-1}\right\}$$

makes it possible to apply the fast Fourier transform algorithm to equations (11). This procedure is called the causal inverse fast Fourier transform (CIFFT) (Hayashi and Katukura, 1990).

Modified CIFFT

Two correction terms $A_I(t)$, $A_R(t)$ can be introduced to equations (11) corresponding with the inverse Fourier transform integral over $\omega_n(=N\Delta\omega/2)<|\omega|<\infty$:

$$S_l^r(t) = 4U(t)\cdot\mathrm{Re}\left[\frac{1}{2\pi}\int_0^{\omega_n}k^r(\omega)e^{\mathrm{i}\omega t}d\omega\right] + A_I(t) = 4U(t)\cdot\mathrm{Re}\left[\frac{1}{2\pi}\int_0^{\omega_n}\mathrm{i}\omega\cdot c^r(\omega)e^{\mathrm{i}\omega t}d\omega\right] + A_R(t). \tag{13}$$

If $k^r(\omega)$ and $\omega\cdot c^r(\omega)$ could be approximately written by the asymptotic form

$$k^r(\omega) = \frac{\omega_n^2\cdot k^r(\omega_n)}{\omega^2}, \qquad \omega\cdot c^r(\omega) = \frac{\omega_n^2\cdot c^r(\omega_n)}{\omega} \tag{14}$$

in $|\omega| > \omega_n$, the correction terms become

$$A_R(t) = 4U(t)\left[\frac{1}{2\pi}\omega_n^2 c^r(\omega_n)\cdot \mathrm{si}(\omega_n t)\right], \qquad A_I(t) = 4U(t)\left[\frac{1}{2\pi}\omega_n k^r(\omega_n)\{\sin\omega_n t + \omega_n t\cdot \mathrm{si}(\omega_n t)\}\right] \tag{15}$$

where si is the sine integral.

Disrete Hilbert Transform (DHT)

If $c^r(\omega)$ is defined at n points $\omega_1, \cdots, \omega_n$, the discrete form of equation (9) is then

$$k^r(\omega_j) = -\frac{2}{\pi}\sum_{\substack{k=1\\(k\neq j)}}^{n}\frac{\omega_k^2\cdot c^r(\omega_k)}{\omega_k^2-\omega_j^2}\Delta\omega \tag{16}$$

in which $\Delta\omega = \omega_k - \omega_{k-1}$ (Simon and Tomlinson, 1984).

Modified DHT

The correction term corresponding to equation (14) can be added to the discrete Hilbert transform (16):

$$k^r(\omega_j) = -\frac{2}{\pi}\sum_{\substack{k=1\\(k\neq j)}}^{n}\frac{\omega_k^2\cdot c^r(\omega_k)}{\omega_k^2-\omega_j^2}\Delta\omega + B_R(\omega_j) \tag{17}$$

in which

$$B_R(\omega_j) = \frac{\omega_n c^r(\omega_n)}{\pi}\cdot\frac{\omega_n}{\omega_j}\cdot\log\frac{\omega_n^*-\omega_j}{\omega_n^*+\omega_j} \quad (0<\omega_j\le\omega_n) \tag{18.a}$$

$$= \frac{\omega_n c^r(\omega_n)}{\pi}\cdot\left(-\frac{2\omega_n}{\omega_n^*}\right) \qquad (\omega_j = 0) \tag{18.b}$$

and $\omega_n^* = \omega_n + \frac{1}{2}\Delta\omega$.

COMPLEX EXPONENTIAL ALGORITHM

The regular part of the dynamic stiffness of soil $S_l^r(\omega)$ can be approximately expressed in a partial-fraction expansion of the form

$$S_l^r(\omega) = \sum_{k=1}^{N_1}\left(\frac{D_k}{\mathrm{i}\omega-\lambda_k}+\frac{D_k^*}{\mathrm{i}\omega-\lambda_k^*}\right)+\sum_{k=1}^{N_2}\frac{C_k}{\mathrm{i}\omega+\gamma_k} \tag{19}$$

where γ_k is real and λ_k^* is the conjugate of a complex number $\lambda_k = -\beta_k + \mathrm{i}\omega_k$. Applying the inverse Fourier transform results in

$$S_l^r(t_m) = 2\mathrm{Re}\left\{\sum_{k=1}^{N_1}D_k X_k^m\right\}+\sum_{k=1}^{N_2}C_k Y_k^m$$

$$= \sum_{k=1}^{N_1} \left(A_k e^{-\beta_k m\Delta T} \cos \omega_k m\Delta T + B_k e^{-\beta_k m\Delta T} \sin \omega_k m\Delta T \right) + \sum_{k=1}^{N_2} C_k e^{-\gamma_k m\Delta T} \tag{20}$$

with $X_k = e^{(-\beta_k + i\omega_k)\Delta T}$, $Y_k = e^{-\gamma_k \Delta T}$ and $A_k = 2\mathrm{Re}[D_k]$, $B_k = -2\mathrm{Im}[D_k]$.

The polynomial of $n(=2N_1 + N_2)$th order with the roots X_k, X_k^*, Y_k is defined as

$$\alpha_n X^n + \alpha_{n-1} X^{n-1} + \cdots + \alpha_1 X + \alpha_0 = \prod_{k=1}^{N_1} (X - X_k)(X - X_k^*) \prod_{k=1}^{N_2} (X - Y_k) = 0 \tag{21}$$

where $\alpha_n = 1$. Multiplying the both sides of equation (20) by α_m and adding it from $m = 0$ to n leads to

$$S_l^r(t_n) + \sum_{m=0}^{n-1} S_l^r(t_m) \cdot \alpha_m = 2\mathrm{Re}\left\{ \sum_{k=1}^{N_1} D_k \left(\sum_{m=0}^{n} \alpha_m X_k^m \right) \right\} + \sum_{k=1}^{N_2} C_k \left(\sum_{m=0}^{n} \alpha_m Y_k^m \right). \tag{22}$$

Considering equation (21) results in

$$\sum_{m=0}^{n-1} S_l^r(t_m) \cdot \alpha_m = -S_l^r(t_n). \tag{23}$$

To determine coefficients α_m, $p(>>n)$ linear equations for $n$unknowns are constructed by using p sets of n discrete points each starting from one delayed point as shown in Fig.2. They can be solved by a generalized inverse technique based on the singular value decomposition. X_k, Y_k and A_k, B_k, C_k are obtained by equation (21) and (20) respectively. This method is called Complex Exponential Algorithm (CEA) (Brown *et al*, 1979) which makes it possible to represent the data of time history by a linear combination of stably dumped harmonic functions.

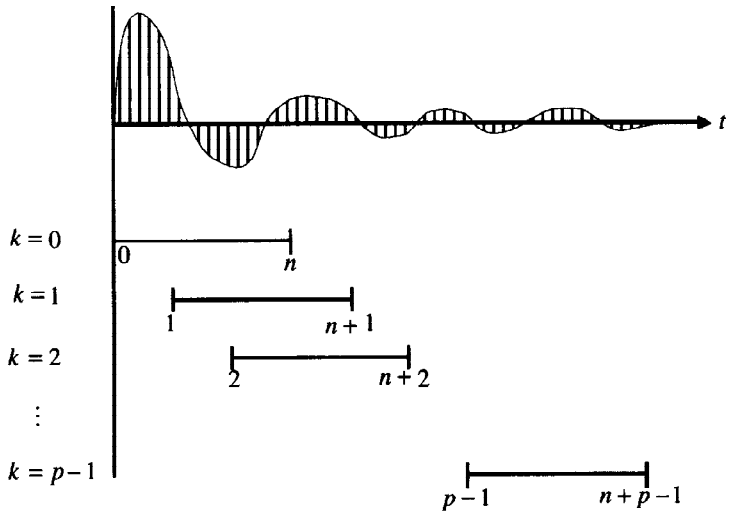

Fig.2 Discrete data in time domain

NUMERICAL EXAMPLE

The semi-infinite rod with exponentially increasing section area (Wolf and Obernhuber, 1985) is considered as the numerical example (Fig.3). The dynamic stiffness of the vertical translation at the top is written as follows:

$$\frac{f}{EA_0}S(a_0)=\frac{1}{2}\left(1+\sqrt{1-4a_0^2}\right)\ :\ a_0=\frac{\omega f}{C_0},\ C_0=\sqrt{\frac{E}{\rho}} \tag{24}$$

where E is the Young's modulus, ρ is the mass density.

Figure 4 shows the impulse function calculated by using equations (13) and (17). Dots denote the exact solution:

$$\frac{f}{EA_0}S_1^r(\tau)=\frac{C_0}{f}\cdot\frac{1}{2\tau}J_1\left(\frac{\tau}{2}\right)\quad :\ \tau=\frac{C_0}{f}t \tag{25}$$

where J_1 is the Bessel function of the first kind and of the first order. Both of numerical and exact results have a good agreement.

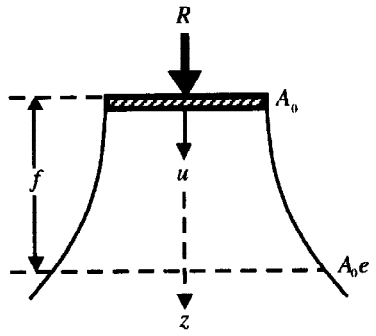

Fig.3 Analytical model

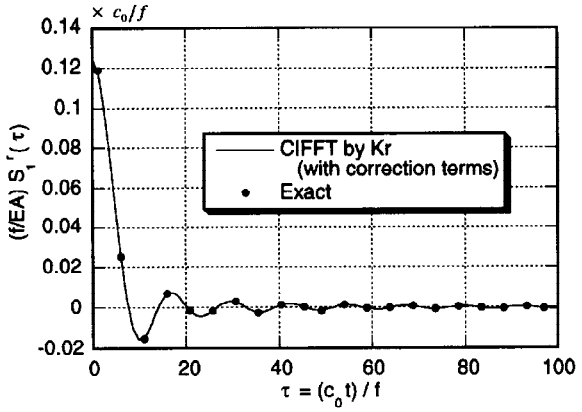

Fig.4 Impulse function of regular part of dynamic stiffness by $\mathrm{Im}[S_1^r(a_0)]$

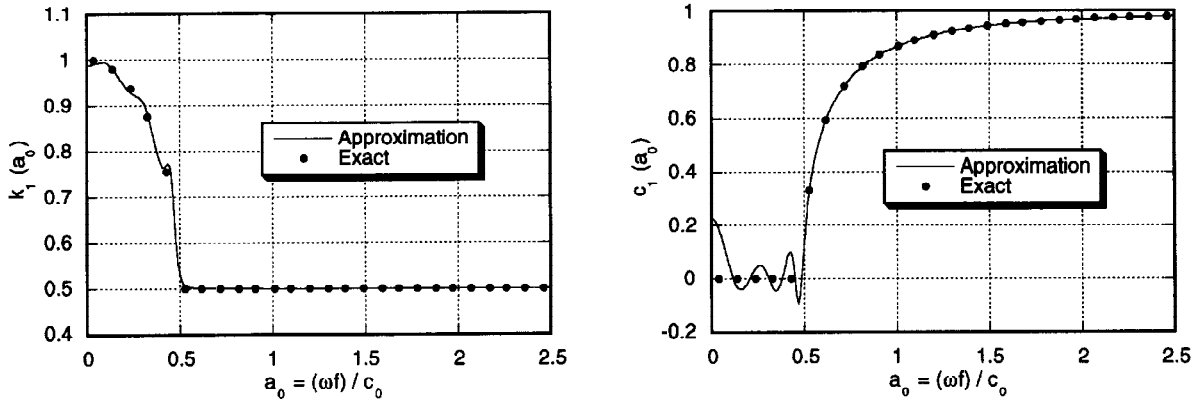

Fig.5 Real part (a) and imaginary part (b) of dynamic stiffness in frequency domain by $\mathrm{Im}[S_1^r(a_0)]$

Figures 5(a) and 5(b) are the numerical results of $k(\omega)$ and $c(\omega)$ evaluated from equation (19) by CEA method (n=10). Figure 6 shows the impulse function of regular part of the dynamic stiffness evaluated by CEA method. Next when the constrained step displacement is given as follows:

$$u(\tau)=\begin{cases}\tau^2(3-\tau) & \tau\le 2\\ 4 & 2\le\tau\end{cases}, \tag{26}$$

the dynamic interaction force $R(\tau)$ is calculated by equation (8) and compared with the exact solution in Fig. 7. One can find out that the numerical results by CEA method in these figures can well approximate each

exact solution respectively.

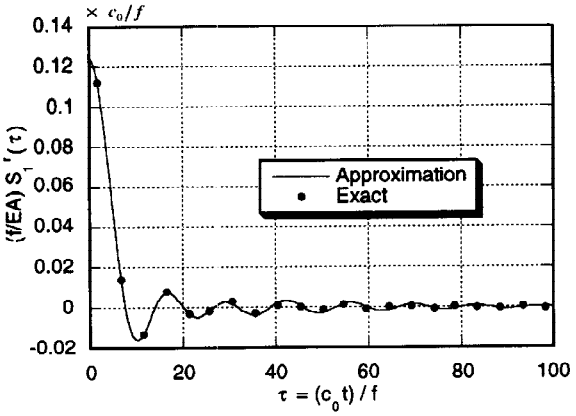

Fig.6 Identification of impulse function of regular part of dynamic stiffness by $\mathrm{Im}[S_1^r(a_0)]$

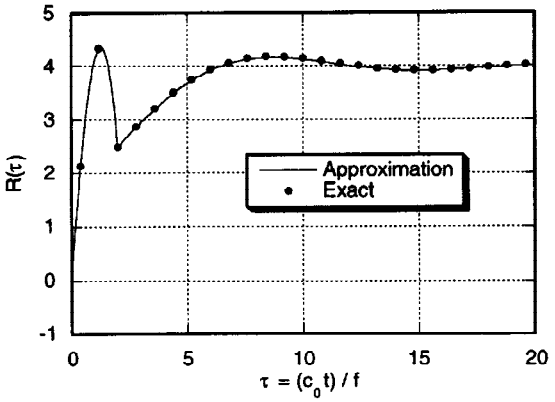

Fig.7 Dynamic interaction force under step displacement

CONCLUDING REMARKS

The modified CIFFT to obtain the impulse function of the dynamic stiffness of soil has been presented. This method becomes more effective to be combined with the modified DHT when the impulse function has to be calculated from the imaginary part of the dynamic stiffness. The obtained data in time history can be expressed by the linear combination of stably dumped harmonic functions by using the CEA method. This method can reduce the storage requirement compared with the ordinarily used FFT.

REFERENCE

Brown, D. L., R. J. Allemang, R. Zimmerman and M. Mergeay (1979). Parameter estimation techniques for modal analysis, *SEA Paper*, No.790221.

Hayashi, Y. and H. Katukura (1990). Effective time-domain soil-structure interaction analysis based on FFT algorithm with causality condition, *Earthquake Engineering and Structural Dynamics*, 19, 693-708.

Simon, M. and G. R. Tomlinson (1984). Use of the Hilbert transform in modal analysis of linear and non-linear structures, *Journal of Sound and Vibration*, 96, No.4, 421-436.

Wijeyewickrema, A. C. and L. M. Keer (1987). Nonlinear antiplane response of rigid inclusion to incident stress wave, *ASCE, Journal of Engineering Mechanics*, 113, No.10, 1565-1583.

Wolf, J. P. and P. Obernhuber (1985). Non-linear soil-structure-interaction analysis using Green's function of soil in the time domain, *Earthquake Engineering and Structural Dynamics*, 13, 213-223.

Wolf, J. P. and G. R. Darbre (1986). Non-linear soil-structure-interaction analysis based on the boundary-element method in time domain with application to embedded foundation, *Earthquake Engineering and Structural Dynamics*, 14, 83-101.

Wolf, J. P. and M. Motosaka (1989). Recursive evaluation of interaction forces of unbounded soil in the time domain, *Earthquake Engineering and Structural Dynamics*, 18, 345-363.

Yoshida, N., Y. Fujitani and D. Fujii (1986). Dynamic soil-foundation interaction analysis based on interrelations of fundamental physical quantities, *Journal of Structural and Construction Engineering*, 367, 103-110 (*in Japanese*).